J|A|C|S
ARTICLES

Interaction between Water-Soluble Peptidic CdSe/ZnS Nanocrystals and Membranes: Formation of Hybrid Vesicles and Condensed Lamellar Phases

Aurélien Dif,[†] Etienne Henry,[‡] Franck Artzner,[‡] Michèle Baudy-Floc'h,[†] Marc Schmutz,[§] Maxime Dahan,[||] and Valérie Marchi-Artzner*[,†]

Sciences Chimiques de Rennes, CNRS UMR 6226, Université Rennes 1, and Institut de Physique de Rennes, CNRS UMR 6251, Université Rennes 1, 35042 Rennes, France, Institut Charles Sadron, CNRS UPR 22, Université Strasbourg 1, 67083 Strasbourg, France, and Laboratoire Kastler Brossel, CNRS UMR 8552, Ecole Normale Supérieure, 75005 Paris, France

Received December 23, 2007; E-mail: valerie.marchi-artzner@univ-rennes1.fr

Abstract: Due to their tunable optical properties and their well-defined nanometric size, core/shell nanocrystals (quantum dots, QDs) are extensively used for the design of biomarkers as well as for the preparation of nanostructured hybrid materials. It is thus of great interest to understand their interaction with soft lipidic membranes. Here we present the synthesis of water-soluble peptide CdSe/ZnS QDs and their interaction with the fluid lipidic membrane of vesicles. The use of short peptides results in the formation of small QDs presenting both high fluorescence quantum yield and high colloidal stability as well as a mean hydrodynamical diameter of 10 nm. Their interaction with oppositely charged vesicles of various surface charge and size results in the formation of hybrid giant or large unilamellar vesicles covered with a densely packed layer of QDs without any vesicle rupture, as demonstrated by fluorescence resonance energy transfer experiments, zetametry, and optical microscopy. The adhesion of nanocrystals onto the vesicle membrane appears to be sterically limited and induces the reversion of the surface charge of the vesicles. Therefore, their interaction with small unilamellar vesicles induces the formation of a well-defined lamellar hybrid condensed phase in which the QDs are densely packed in the plane of the layers, as shown by freeze-fracture electron microscopy and small-angle X-ray scattering. In this structure, strong undulations of the bilayer maximize the electrostatic interaction between the QDs and the bilayers, as previously observed in the case of DNA polyelectrolytes interacting with small vesicles.

Introduction

The interaction between nanosized particles and fluid membranes is involved in many biological phenomena, such as the entry of a virus into a cell, cell signalling, and lipid reorganization in membranes, and plays a crucial role in drug delivery. The ability of nanoparticles to label, target, and penetrate cell membranes is of great interest in studying vesicle trafficking, visualizing lipid or protein in-plan reorganization within the membrane, and understanding the fusion process. The interaction of nanoparticles with lipidic and biological membranes can also be related to their possible toxicity through their nonspecific adhesion and the change in membrane morphology or permeability. In addition, the adsorption of nanoparticles at fluid−fluid interfaces can be used for the fabrication of hierarchical self-assemblies.[1] The first step toward the control of the interaction of nanoparticles in contact with fluid membranes concerns their adhesion. Therefore, our approach is to investigate the interaction between functionalized water-soluble quantum dots (QDs) and vesicles as a fluid model membrane by taking advantage of the optical properties and the versatility of the peptide chemical grafting of QDs.[2,3] Ligand-stabilized semiconductor QDs, which are extensively developed as biolabels, appear very attractive. Inorganic core/shell CdSe/ZnS nanocrystals (QDs) possess a range of tunable optical properties, whereas the surface ligands can be tuned to tailor interactions with the surroundings. The interaction between giant vesicles and gold nanoparticles of diameter around 20 nm was previously found to be drastically dependent on the chemical grafting method used, resulting in either adsorption of the nanoparticles onto the membrane surface or budding and fission of the vesicle induced by lipid exchange (data not shown). Here, our aim is to explore the interaction between nanoparticles and vesicle membranes to induce membrane reorganization or to build self-organized hybrid assemblies. Therefore, bioactivable functionalized QDs of the smallest size possible were prepared by optimizing the chemical surface coating and taking advantage of the properties of the optical QDs to follow their interaction with vesicles of various sizes. In addition, QDs display extremely high extinction coefficients and narrow emission bands over a wide range of wavelengths. These properties make QDs excellent energy

[†] Sciences Chimiques de Rennes, Université Rennes 1.
[‡] Institut de Physique de Rennes, Université Rennes 1.
[§] Université Strasbourg 1.
[||] Ecole Normale Supérieure.

(1) Lin, Y.; Skaff, H.; Emrick, T.; Dinsmore, A. D.; Russell, T. P. *Science* **2003**, *299*, 226–229.
(2) Pinaud, F.; King, D.; Moore, H. P.; Weiss, S. *J. Am. Chem. Soc.* **2004**, *126*, 6115–6123.
(3) Iyer, G.; Pinaud, F.; Tsay, J.; Weiss, S. *Small* **2007**, *3*, 793–798.

10.1021/ja711378g CCC: $40.75
Published on Web 06/05/2008

donors in fluorescence resonance energy transfer (FRET),[4] a technique that is ideally suited for events occurring at the nanometer scale, such as the interaction of QDs with lipidic membranes. As the FRET efficiency drops off with the distance between the donor−acceptor pair as r^6, the chemical layer of the functionalized QDs hinders the possibility of FRET and therefore has to be as thin as possible. The FRET experiments were previously reported to study the interaction between the QD surface and an acceptor chromophore. For example, fluorescence energy transfer was described in the case of the direct binding of the Cy5-labeled maltose histag protein (acceptor) to the QD surface through the histag residue.[5] It was also reported that hydrophobic QDs embedded in a vesicle membrane exhibited FRET with a fluorescent lipid.[6]

Here, the synthesis of water-soluble peptidic QDs of a mean diameter around 10 nm is presented as well as their selective interaction with oppositely charged vesicles. The interaction between these small peptidic QDs and the oppositely charged membrane results in the formation of stable hybrid vesicles and condensed phases that were analyzed by optical and electron microscopies, small angle X-ray scattering (SAXS) as well as zetametry and fluorimetry. In addition, the synthesis of the peptidic functionalized CdSe/ZnS QDs was optimized to reduce, as soon as possible, their final size and to optimize their colloidal stability and their ability to be bioactivable. To quantify the adhesion of QDs, FRET experiments between the QDs used as donor and the vesicle membrane labeled with a rhodamine lipid (Rh-DPPE) used as acceptor are successfully realized.

Results and Discussion

Synthesis of the Functionalized Water-Soluble Quantum Dots. All the experimental methods and materials are described in detail in the Supporting Information.[7–15] A versatile and simple chemical method is required to solubilize and functionalize QDs in water to investigate the interaction between QDs and fluid membranes. We first prepared hydrophobic CdSe/ZnS QDs according to the literature. Various molecular grafting methods based on ligand exchange,[2,16] micellization by amphiphiles,[8,17,18] or polymer coating[19] have been previously described. In particular, phytochelatin-derivated peptides bearing a sequence rich in cystein were successfully used for the bioactivation of CdSe/ZnS QDs resulting from the specific interaction between several cystein residues and the ZnS surface.[2,20] Polyhistidine residues strongly interact with the atoms of Zn and S at the surface of QDs.[21] Therefore, a polyhistidine peptide was recently used as ligand for coating QDs.[6] The described methods resulted in the formation of functionalized water-soluble QDs with a mean hydrodynamic diameter of around 10−20 nm. Here we selected a set of synthetic short peptides bearing an adhesion domain that could interact with the ZnS surface because of cystein's or histidine's affinity for Zn and S atoms, to decrease the final size of the functionalized water-soluble QDs. Size is a crucial parameter for in vivo applications.[22] In addition, a peptidic sequence of biological interest can be grafted on the terminal chemical function of the peptide. For example, a peptide with a bioactive RGD sequence that selectively recognized integrin proteins involved in cell adhesion is prepared.[23] A series of peptides bearing a terminal charged group of various charge, such as a glycine, a lysine, an aspartic acid residues, or its azaβ-3 analogue are synthesized. The efficiency of the peptides for coating nanoparticles is first evaluated in terms of colloidal stability, size, and water solubility of the peptide-QDs by complementary techniques such as dynamic light scattering (DLS), size exclusion high-performance liquid chromatography (SE-HPLC), and electrophoresis. Initially, the hydrophobic QDs are stabilized by trioctylphosphine oxide (TOPO) ligands that are exchanged in the presence of a peptide excess under basic conditions as previously described.[2] The QDs are solubilized into the aqueous phase. After removal of the excess peptide by dialysis, the QDs' purity was controlled by SE-HPLC (see Supporting Information, Figure A). The hydrodynamic diameters of the various peptide-QDs are estimated by DLS to be around 10 nm for the smallest peptide-QDs (see Table 1). The colloidal stability over time of

Table 1. Hydrodynamic Diameter D_h (Mean ± SD) Obtained by DLS[a]

peptide	QD_{535}-peptide	$D_h \pm$ SD (nm)	$l_{min}-l_{max}$ (nm)
1	CCCSSS^{N}azaD	9 ± 1	1.2−2.8
2	CCCSSSG	11 ± 1	1.05−2.5
3	HHHHHHSGSGSGD	12 ± 1.5	1.5−3.5
4	CCCSSSD	10 ± 1.3	1.05−2.45
5	CCCSSSRGD	17 ± 1.5	1.35−3.15

[a] The inorganic diameter d_{QD}, corresponding to the inorganic core/shell of the functionalized nanocrystals QD_{535}, is found to be 4.0 ± 1.5 nm from TEM images,[8] and the theoretical mean diameter of the CdSe nanocrystals is 2.8 nm, calculated from the absorption spectrum according to the literature.[24] The minimal (l_{min}) and maximal (l_{max}) lengths of the peptides are calculated from the lengths of one amino acid respectively incorporated into an α-helix (1.5 Å/peptide) and a β-sheet (3.5 Å/peptide) structured peptide sequence.

(4) Pons, T.; Medintz, I. L.; Wang, X.; English, D. S.; Mattoussi, H. *J. Am. Chem. Soc.* **2006**, *128*, 15324–15331.
(5) Medintz, I. L.; Clapp, A. R.; Mattoussi, H.; Goldman, E. R.; Fisher, B.; Mauro, J. M. *Nat. Mater.* **2003**, *2*, 630–638.
(6) Delehanty, J. B.; Medintz, I. L.; Pons, T.; Brunel, F. M.; Dawson, P. E.; Mattoussi, H. *Bioconjugate Chem.* **2006**, *17*, 920–927.
(7) Dabbousi, B. O.; RodriguezViejo, J.; Mikulec, F. V.; Heine, J. R.; Mattoussi, H.; Ober, R.; Jensen, K. F.; Bawendi, M. G. *J. Phys. Chem. B* **1997**, *101*, 9463–9475.
(8) Boulmedais, F.; Bauchat, P.; Brienne, M. J.; Arnal, I.; Artzner, F.; Gacoin, T.; Dahan, M.; Marchi-Artzner, V. *Langmuir* **2006**, *22*, 9797–9803.
(9) Yu, W. W. Q., L.; Guo, W.; Peng, X. *Chem. Mater.* **2003**, *15*, 2854.
(10) Schmidt, R.; Schmutz, M.; Michel, M.; Decher, G.; Mésini, P. J. *Langmuir* **2002**, *18*, 5668–5672.
(11) Marchi-Artzner, V.; Brienne, M. J.; Gulik-Krzywicki, T.; Dedieu, J. C.; Lehn, J. M. *Chem.-Eur. J.* **2004**, *10*, 2342–2350.
(12) Marchi-Artzner, V.; Gulik-Krzywicki, T.; Guedeau-Boudeville, M. A.; Gosse, C.; Sanderson, J. M.; Dedieu, J. C.; Lehn, J. M. *Chemphyschem* **2001**, *2*, 367–376.
(13) Angelova, M. I.; Dimitrov, D. S. *Mol. Cryst. Liq. Cryst.* **1987**, *152*, 89–104.
(14) Van Grondelle, W.; et al. *J. Struct. Biol.* **2007**, *160*, 211–223.
(15) Narayanan, T.; Diat, O.; Bosecke, P. *Nucl. Instrum. Methods* **2001**, *467*, 1005–1009.
(16) Susumu, K.; Uyeda, H. T.; Medintz, I. L.; Pons, T.; Delehanty, J. B.; Mattoussi, H. *J. Am. Chem. Soc.* **2007**, *129*, 13987–13996.
(17) Dubertret, B.; Skourides, P.; Norris, D. J.; Noireaux, V.; Brivanlou, A. H.; Libchaber, A. *Science* **2002**, *298*, 1759–1762.
(18) Dubois, F.; Mahler, B.; Dubertret, B.; Doris, E.; Mioskowski, C. *J. Am. Chem. Soc.* **2007**, *129*, 482–483.
(19) Luccardini, C.; Tribet, C.; Vial, F.; Marchi-Artzner, V.; Dahan, M. *Langmuir* **2006**, *22*, 2304–2310.
(20) Bontidean, I.; Ahlqvist, J.; Mulchandani, A.; Chen, W.; Bae, W.; Mehra, R. K.; Mortari, A.; Csoregi, E. *Biosens. Bioelectron.* **2003**, *18*, 547–553.
(21) Sapsford, K. E.; Pons, T.; Medintz, I. L.; Higashiya, S.; Brunel, F. M.; Dawson, P. E.; Mattoussi, H. *J. Phys. Chem. C* **2007**, *111*, 11528–11538.
(22) Liu, W.; Choi, H. S.; Zimmer, J. P.; Tanaka, E.; Frangioni, J. V.; Bawendi, M. *J. Am. Chem. Soc.* **2007**, *129*, 14530–14531.
(23) Marchi-Artzner, V.; Lorz, B.; Gosse, C.; Jullien, L.; Merkel, R.; Kessler, H.; Sackmann, E. *Langmuir* **2003**, *19*, 835–841.

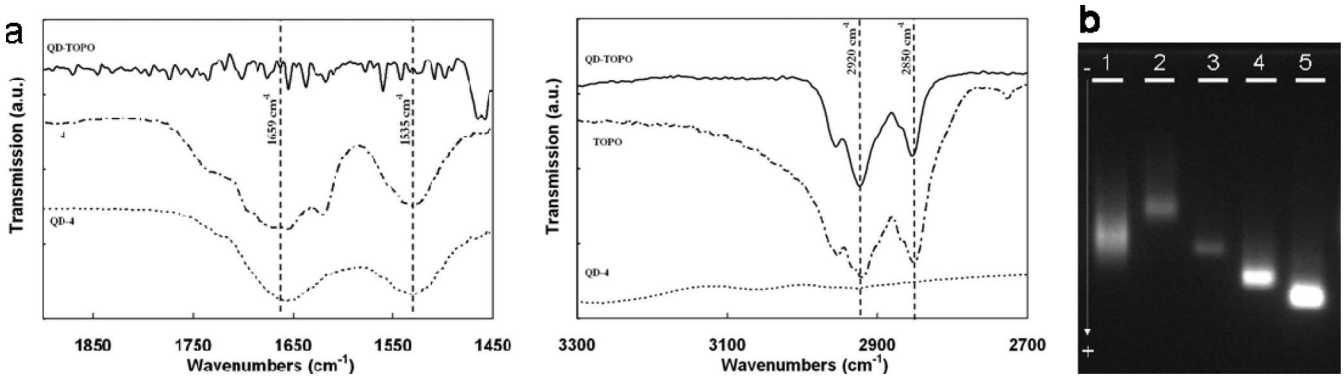

Figure 1. (a) FT-IR spectra of QD_{535}-TOPO (—), QD_{535}-**4** (•••), and peptide **4** and TOPO (—•—) as a KBr pellet. (b) 1% Agarose electrophoresis gel of QD_{535} grafted with peptides **1**−**5** in PBS buffer at pH 7.4.

the QDs is very high (several months at 4 °C) in the case of **1**, **2**, and **4**, whereas peptides **3** and **5** tend to form some aggregates with time (up to two weeks). As expected from the chemical structure, the sizes of the peptide-QDs with **1**, **2**, and **4** are small.

The FT-IR spectra of the purified QD_{535}-**4** and QD_{535}-TOPO have been recorded, as well as those of peptide **4** and TOPO alone. The presence of peptide **4** on the QDs is confirmed by two peaks assigned to amide II and I bonds at 1535 and 1659 cm^{-1}, respectively. In the case of the pure peptide **4**, the later positions of the amide vibration bands indicated a β-sheet structure. Conversely, the peptide exhibits a random structure at the surface of the QDs (see Figure 1a). In addition, no trace of TOPO is observed after the peptides are grafted on the QD surface, as indicated by the absence of peaks assigned to the methylene vibration at 2920 and 2850 cm^{-1}. Because of their well-defined small size, the peptide-QDs can migrate easily as sharp and well-defined fluorescent spots on electrophoresis gel (see Figure 1b). This feature is particularly suitable for coupling the QDs to biomolecules.

To evaluate the efficiency of the functionalization, the optical and colloidal properties of the peptide-QD are investigated. The absorbance and photoluminescence spectra of the QDs are recorded before and after functionalization and purification. The emission spectrum of the QD_{535}-**4** nanocrystals after functionalization exhibits a 5 nm bathochromic shift of the emission peak, attributed to a change of the electronic structure of the ZnS surface coated with the peptide. The photoluminescence intensity is decreased around 30% after the peptide grafting (see Figure 2). Similar results have been observed with thiols, thiocarbamates,[18] and phytochelatin peptidic ligands.[2,25,26] The fluorescence quantum yields of QD_{535}-TOPO and QD_{535}-**4** are found to be 40% and 24%, respectively, by using as reference the rhodamine 6G chromophore.

No change in the photoluminescence intensity and hydrodynamic diameter is observed in the presence of a strong ionic strength up to 0.5 M (see Supporting Information, Figure B). In addition, the peptide-QDs can be stored as a lyophilized powder and redispersed in water without any significant aggregation, as demonstrated by DLS measurements.

In conclusion, the small peptides used provide a simple way to prepare water-soluble functionalized QDs with a high colloidal stability, efficient optical properties, and a very small hydrodynamical diameter of about 10 nm, comparable to the smallest water-soluble QDs previously described.[3,27]

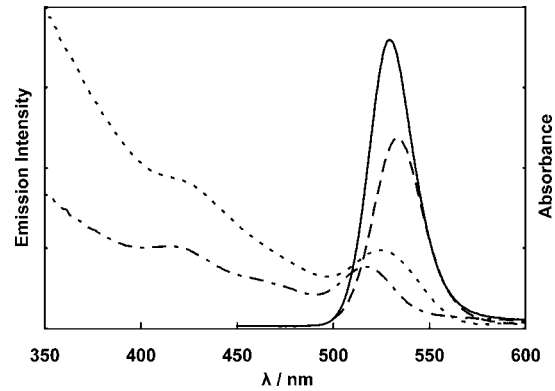

Figure 2. Normalized emission intensity of (—) QD_{535}-TOPO solubilized in toluene before functionalization (emission peak at 535 nm) and (— —) peptide-coated QD_{535}-**4** solubilized in water (emission peak at 540 nm). The excitation wavelength was 350 nm. The corresponding UV spectra of (—•—) QD_{535}-TOPO and (•••) peptide-coated QD_{535}-**4** are also shown.

Interaction with Oppositely Charged Vesicles. The interaction of these negatively charged water-soluble peptide-QDs with oppositely charged vesicles of various sizes, used as a fluid model membrane, is investigated to understand how small (nanometric), soluble nanocrystals can interact with a fluid membrane and to build new hybrid molecular assemblies. The electrostatic interaction is the most efficient nonspecific interaction to induce adhesion onto a fluid membrane. First, the interaction with giant unilamellar vesicles (GUVs) was observed by optical dark-field and fluorescence microscopies. The QD_{535}-**4** solution is added under microscope to an iso-osmolar solution of neutral (pure EPC) or positively charged (DOTAP/EPC (5:95)) giant unilamellar vesicles (GUV+). The contact of the two solutions results in a diffusive concentration gradient of QD_{535}-**4** into GUV and can be measured from the fluorescence level. When the fluorescent front comes into contact with the vesicles, two distinct behaviors occur, depending on the vesicle charge: the membrane of the GUV+ vesicles appears homogeneously fluorescent in less than 1 min (Figure 3b), whereas no fluorescence is observed for the neutral vesicles (see Figure 3c). This observation is attributed to the selective adhesion of QD_{535}-**4** onto the oppositely charged vesicle surface.

(24) Yu, W. W.; Qu, L. H.; Guo, W. Z.; Peng, X. G. *Chem. Mater.* **2003**, *15*, 2854–2860.
(25) Pinaud, F.; Michalet, X.; Bentolila, L. A.; Tsay, J. M.; Doose, S.; Li, J. J.; Iyer, G.; Weiss, S. *Biomaterials* **2006**, *27*, 1679–1687.
(26) Tsay, J. M.; Doose, S.; Pinaud, F.; Weiss, S. *J. Phys. Chem. B* **2005**, *109*, 1669–1674.
(27) Pons, T.; Uyeda, H. T.; Medintz, I. L.; Mattoussi, H. *J. Phys. Chem. B* **2006**, *110*, 20308–20316.

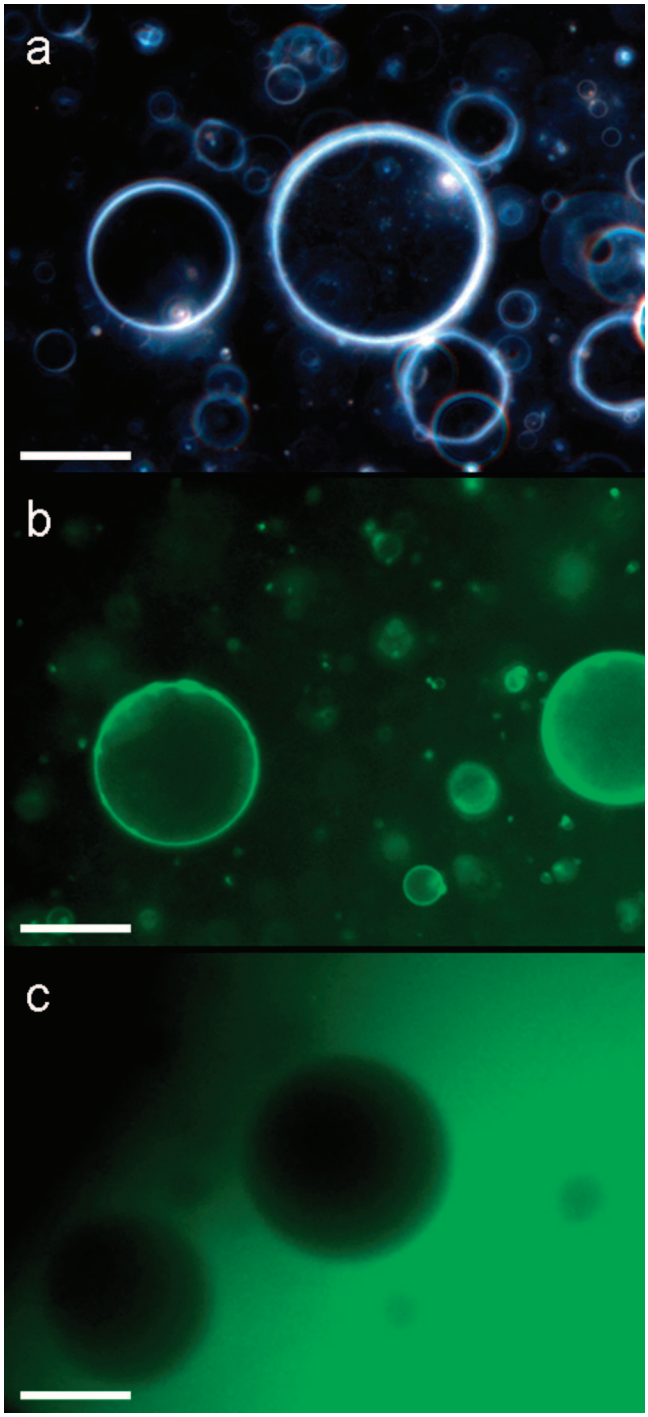

Figure 3. Optical microscopy images of (a) positively charged DOTAP/EPC (5:95) GUV+ observed in dark field, (b) negative QD-**4** (0.1 μM) put in contact with positively charged DOTAP/EPC (5:95) GUV+ observed in fluorescence, and (c) negative QD-**4** (0.1 μM) put in contact with neutral EPC GUV observed in fluorescence. The scale bar represents 10 μm.

The vesicles keep their integrity; furthermore, the membrane fluctuations due to the Helfrich undulations, which are visible on the dark-field image in the case of free GUV+, vanish once the membrane becomes fluorescent. Thus, QD_{535}-**4** selectively adhere onto oppositely charged vesicles via electrostatic interaction and inhibits their fluctuations; therefore, the QDs appear to rigidify the vesicle membrane and reduce the surface excess of membranes.

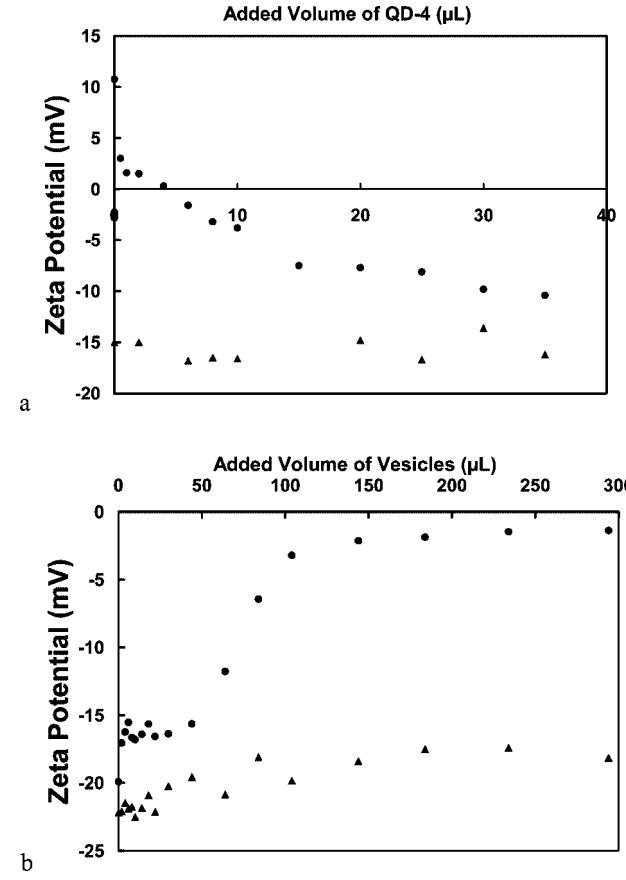

Figure 4. (a) Zeta potential (ζ) as a function of the added volume V of QD_{535}-**4** (1.1 μM) during the titration of a solution of vesicle (LUV+, 0.133 mM, 0.6 mL): ●, LUV+; ▲, LUV EPC. (b) Zeta potential as a function of the added volume V of positively charged vesicles (LUV+, 1.33 mM) during the titration of a solution of QD_{535}-**4** (1.1 μM, 0.6 mL): ●, LUV+; ▲, LUV EPC. The titrations are performed in the presence of 50 mM NaCl.

To get more information on the mechanism of the interaction between QDs and giant vesicles, a QD_{535}-**4** solution is titrated with a solution of DOTAP/EPC (5:95) cationic large unilamellar vesicles (LUV+) of a mean diameter of 100 nm, and conversely (see Figure 4). The zeta potential (ζ) during the two symmetrical LUVs/QD_{535}-**4** titrations is measured in order to follow the evolution of the vesicle surface charge.[27] The mean of the zeta potentials measured in the case of a colloidal mixture is expected to be dependent upon the experimental setup. In the present case, the zeta potential is estimated from the autocorrelation function that enhances the events with short characteristic time. Therefore, the contribution of the free QD_{535}-**4** (10 nm hydrodynamic diameter) is expected to be higher than that of the vesicles (hydrodynamic diameter 100 nm) because QDs are moving faster. In addition, the contribution of the hybrid vesicles (LUV-QD) is expected to be higher than the contribution of free vesicles (LUV) during the titration, due to their higher refractive index.

In the titration of LUV+ by QD_{535}-**4** shown in Figure 4a, the zeta potential ζ_{LUV+} of the LUV+ solution is found to be +12 mV at the beginning of the titration. In presence of a vesicle excess, the mean zeta potential decreases, and this trend is reversed with the addition of negatively charged of QD_{535}-**4**. On the curve, the zeta potential is equal to zero for a volume of 4 μL of QD_{535}-**4** (1.1 μM). At this point, the number of negative QD_{535}-**4** per positive DOTAP lipid on the outer leaflet is evaluated to be 1/450. This neutralization is reached at a very

low QD/DOTAP ratio, indicating that the QDs are highly charged. Taking into account the charges of the C-terminal aspartic acid, the peptide **4** is twice negatively charged at pH 7. Considering the QD_{535} as an inorganic rigid sphere of 4 nm diameter and assuming that the mean molecular area per peptide **4** is at least the cross section of a β-sheet (0.5 nm^2), coating the QD_{535} surface requires less than 100 peptides. Therefore, one can estimate that there are less than 200 negative charges per QD_{535}-**4**. Once the vesicle charge is neutralized, the mean zeta potential still decreases, resulting in a charge reversion of the vesicles with a plateau around −10 mV (see Figure 4a). As an additional experiment, the titration of twice more concentrated vesicles (LUV+) with QD-**4** is performed. The volume of QD required to neutralize the vesicles is found to be proportional to the initial amount of vesicles (see Supporting Information, Figure C).

This titration clearly demonstrates that the interaction between vesicles induces a neutralization and even a reversion of the vesicle charges.

In the case of the symmetrical titration reported in Figure 4b, the negative zeta potential of the QD_{535}-**4** solution is initially found to be −15 mV and remains constant until the point corresponding to a volume of 50 μL of added vesicles (LUV+). In an excess of QDs, the mean zeta potential values are imposed by the free QD_{535}-**4** until all the free QD_{535}-**4** is consumed by interacting with vesicles. For 50 μL of LUV+, the number of QD_{535}-**4** per lipids of the outer leaflet is around 50. From a volume of 50 to 100 μL of added LUV+, the absolute value of the zeta potential decreases until reaching a plateau around −3 mV, the zeta potential remaining always negative. This final value indicates that the formed hybrid vesicles (LUV-QD) are negatively charged, which is attributed to an excess of negative charges coming from the adhering QDs. The control titration performed with neutral vesicles confirms that the interaction between QDs and the vesicles is electrostatically driven.

The same titration was followed by fluorescence with a solution of DOTAP/EPC/Rh-DPPE (5:94.5:0.5)-labeled large unilamellar vesicles (LUV Rh+). In principle, the adhesion of QDs onto vesicles could be detected from the fluorescent resonance energy transfer (FRET) with the QDs as a donor and the rhodamine lipid as an acceptor.[28] During the titration of the QD_{535}-**4** with the positive LUV Rh+, a strong decrease of the QD emission intensity at 530 nm was observed until a plateau is reached, whereas the acceptor rhodamine emission intensity at 590 nm increases (see Figure 5a). [Note: The direct excitation of the rhodamine acceptor was substracted from all the spectra in Figure 4a.] As reported in Figure 5b, the decrease in normalized emission intensity of the QD, acting as a donor, is found to be around 60% in the case of oppositely charged vesicles LUV+ and only 20% in the control experiment performed with neutral EPC/Rh-DPPE (99.5:0.5) LUV+. In the presence of a vesicle excess, e.g., at the end of the titration, the emission intensity reached a plateau corresponding to the saturation of the vesicle surface for about 100 μL of added LUV+. In a dilute regime of vesicles, if one considers that each added vesicle is immediately saturated with QD_{535}-**4**, as suggested from the experiments performed on GUV+ and by zetametry, then there must be two species present: free QD_{535}-**4** and the formed hybrid vesicles (LUV-QD). In such a case, the emission intensity of the QDs is expected to decrease linearly

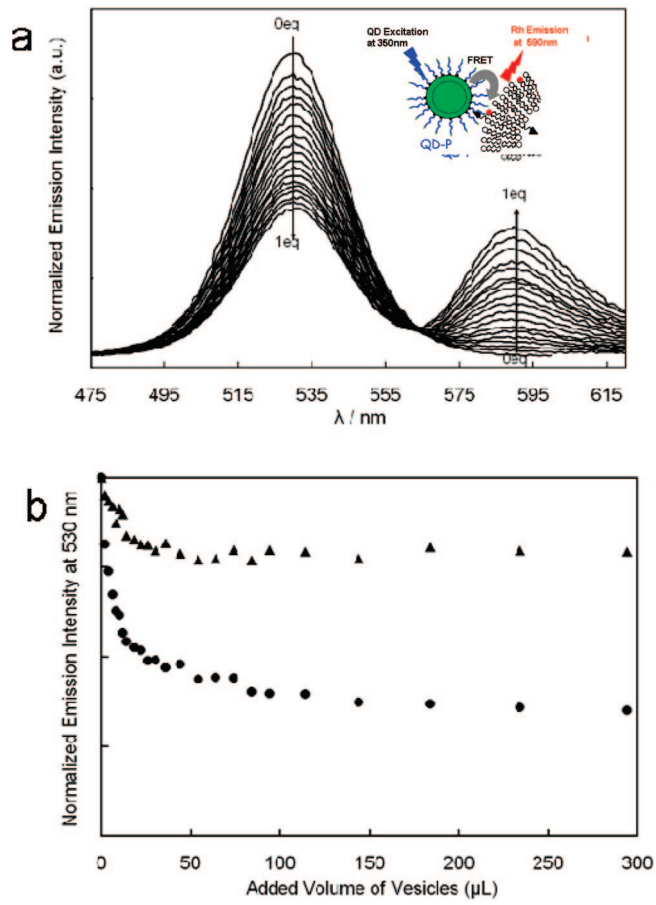

Figure 5. Principle of the FRET experiment between positively charged DOTAP/EPC/Rh-DPPE (5:94.5:0.5) vesicles (LUV Rh+ as an acceptor) and negatively charged peptide-coated QD_{535}-**4** as a donor. (a) Fluorescence emission spectra arising from titration of 0.600 mL of a solution of QD_{535}-**4** (1.1 μM) by a solution of 1.33 mM of positively charged vesicles (LUV Rh+) in 50 mM glucose (λ_{exc} = 350 nm). (b) Corresponding normalized fluorescence intensity $I_f(V)/I_f(0)$ as a function of the volume V of the solution of 1.33 mM of positively charged vesicles (LUV Rh+): ●, LUV +; ▲, LUV EPC (λ_{exc}= 350 nm, λ_{em}= 530 nm).

as the population of hybrid vesicles (LUV-QD) increases, as observed in Figure 4b. One can estimate the distance between the QDs interacting on the vesicle surface. Taking a mean molecular area per lipid of 0.6 nm^2 and considering that QDs are densely packed in a hexagonal arrangement on the vesicle surface, the distance between QDs is 7.2 nm for 75 μL of LUV+. This estimation is in agreement with a densely packed layer of QDs of diameter around 7 nm at the vesicle surface. This value is intermediate between the diameter of the inorganic core/shell nanocrystal observed by TEM (4.0 nm) and the mean hydrodynamical diameter (10 nm) taking into account the ligand and the solvatation layer. The resulting hybrid vesicles are negatively charged and present a densely packed QD layer on the surface.

In conclusion, the zeta potential and fluorimetry titrations demonstrate that the charge neutralization of the vesicles occurs during QD_{535}-**4** adhesion. The final hybrid vesicles (LUV-QD) are negatively charged; therefore, a charge reversion of the vesicles results from the titration. The equilibrium point does not correspond to the charge neutralization of the vesicles but more certainly to the steric saturation of the vesicle surface with QDs. The adsorption of QDs onto the membrane is thus limited by steric hindrance. The electrostatic repulsions between

(28) Clapp, A. R.; Medintz, I. L.; Mattoussi, H. *ChemPhysChem* **2006**, *7*, 47–57.

Table 2. X-ray Data of Hybrid Structures Composed of Lipids and QD-**4**

	lipids	λ_{em}, QD concentration	d_{lam} (Å)[a]	q_{exp} (q_{theo}) (Å^{-1})	T (°C)
1	EPC	−	63.5	0.100 (0.099) 0.197 (0.198)	20
2	EPC/DOTAP (90:10)	600nm,1μM	78.5	0.080 (0.080) 0.160 (0.160)	20
3	DMPC/DMTAP (90:10)	545nm,5μM	80.5	0.078 (0.078) 0.156 (0.156) 0.234 (0.233) 0.310 (0.311)	20
4	DMPC/DMTAP (90:10)	600nm,5μM	86.7	0.072 (0.073) 0.145 (0.145) 0.218 (0.218)	20
5	DMPC/DMTAP (90:10)	600nm,1μM	78.9 110	0.080 (0.080) 0.159 (0.159) 0.057[c]	20
6	DMPC/DMTAP (95:5)	600nm,5μM	93.8 114	n.o.[b] (0.067) 0.135 (0.134) 0.199 (0.200) 0.055[c]	20
7	DMPC/DMTAP (95:5)	600nm,5μM	89.5 139	0.070 (0.070) 0.141 (0.140) 0.210 (0.210) 0.045[c]	45

[a] d_{lam} is the repeat distance of the lamellar structures calculated from the theoretical peak indexation (q_{theo}) of the experimental peak position (q_{exp}). [b] Not observed. [c] Additional peak due to the order of QDs superstructure.

neighboring adhered QDs are not the predominant force that limits the number of adhered QDs.

As the electrostatic interaction between vesicles and peptide QD_{535}-**4** results in a charge reversion of the vesicles, QD_{535}-**4** and hybrid vesicles (LUV-QD) can further interact to form condensed hybrid phases stabilized by electrostatic forces, as observed in the case of a mixture of DNA macromolecules and cationic lipids.[29] Therefore, small unilamellar vesicles of various surface charges (SUV+) composed of an EPC/DOTAP (90:10) mixture are prepared and incubated in the presence of QD-**4** of various size. SUVs of 20−40 nm diameter are well known to easily rupture due to the strong membrane curvature. The resulting fuzzy precipitate is analyzed by small angle X-ray scattering (SAXS). Two peaks are observed (Table 2, entries 1 and 2) and should be attributable to a multilamellar organization, but they are not enough clear to definitively conclude this. The interaction with other peptides or amphiphiles is tested to select the birefringent and organized phases. The peptide **4** is identified as the best compound to form well-defined structures. In addition, this peptide provides the best quality of solubilized and negatively charged QDs in terms of colloidal stability and monodispersity.

By replacing EPC with DMPC lipid, for which the alkyl chains are in a crystalline state at room temperature, one can observe the formation of a birefringent phase (see Figure 6a) for the mixture QD_{545}-**4**/(DMPC/DMTAP 90:10) SUV+. This cationic lipid mixture is known to form well-organized lamellar structures in the presence of anionic colloids such as DNA.[30] DMPC/DMTAP SUVs with various surface charges at a concentration of 20 mg/mL were mixed with anionic QDs of two distinct sizes (QD_{545}-**4** and QD_{600}-**4**) and various concentrations (see Figure 6d). If the QD excess is high, then discrete and fine peaks are observed in the X-ray spectra that are indexed in a multilamellar structure with a lamellar repeat distance which increases with the size of the QDs (Table 2, entries 3 and 4; Supporting Information, Figure D). The repeat distances are larger than those observed in pure lipids, and QDs are thus embedded between lipidic bilayers, as observed with anionic DNA.[30,31] In the case of polyelectrolytes such as DNA or dextran sulfate, the membranes are flat, and the repeat distance is consequently approximately the sum of the bilayer thickness and the polyelectrolyte diameter.[32] In the present case, such a model is not valid since the sum of the bilayer thickness e_{lip}, about 4.8 nm,[33] and the coated QDs diameter d_{QD}, about 6−10 nm, is not compatible with the observed the repeat distance d_{lam} of about 8 nm. The only possibility to reduce the apparent repeat distance is to let the membrane freely undulate, as observed with DNA[30] or actin polyelectrolyte;[34] a model is proposed as shown in Figure 6c.

In this model, the repeat distance is the sum of half the QD diameter and the thickness of one bilayer. $d_{lam} = d_{QD}/2 + e_{lip}$. With $e_{lip} = 4.8$ nm,[35] the QD diameters should be evaluated from the X-ray experiments to be 8.1 nm for QD_{545}-**4** and 9.3 for QD_{600}-**4**. These values strongly support the very small size of the QD coated by a single layer of peptides and the model

(29) Zantl, R.; Artzner, F.; Rapp, G.; Radler, J. O. *Europhys. Lett.* **1999**, *45*, 90–96.
(30) Artzner, F.; Zantl, R.; Rapp, G.; Radler, J. O. *Phys. Rev. Lett.* **1998**, *81*, 5015–5018.
(31) Radler, J. O.; Koltover, I.; Salditt, T.; Safinya, C. R. *Science* **1997**, *275*, 810–814.
(32) Artzner, F.; Zantl, R.; Rädler, J. O. *Cell. Mol. Biol.* **2000**, *46*, 967–978.
(33) Tristram-; Nagle, S.; Liu, Y.; Legleiter, J.; Nagle, J. F. *Biophys. J.* **2002**, *83*, 3324–3335.
(34) Wong, G. C. L.; Tang, J. X.; Lin, A.; Li, Y. L.; Janmey, P. A.; Safinya, C. R. *Science* **2000**, *288*, 2035–2039.
(35) Zantl, R.; Baicu, L.; Artzner, F.; Sprenger, I.; Rapp, G.; Rädler, J. O. *J. Phys. Chem. B* **1999**, *103*, 10300–10310.

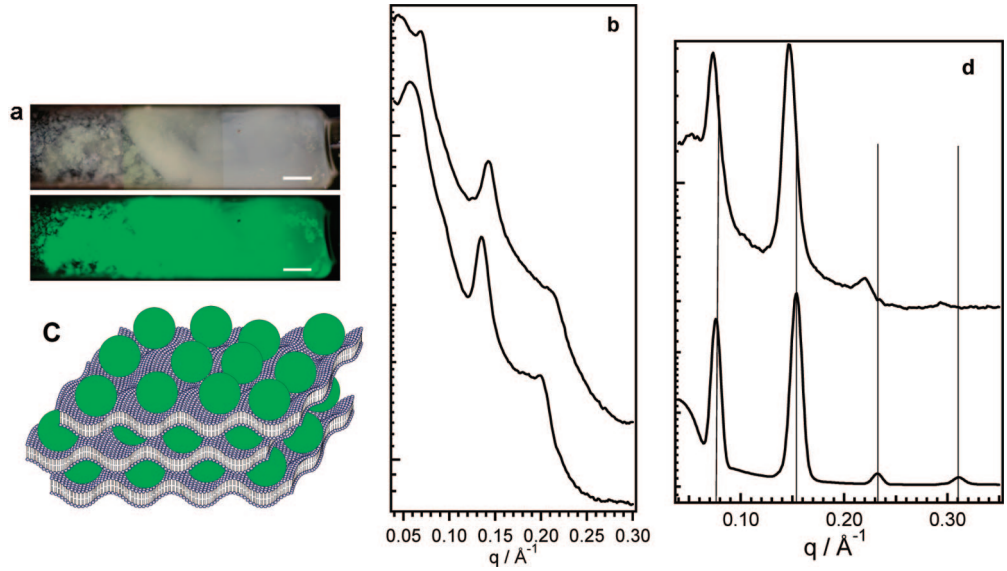

Figure 6. (a) Optical microscopy images of a mixture of QD_{545}-**4**/(DMPC/DMTAP 90:10) SUV+ observed by polarized light (top) and fluorescence (bottom). Note the birefringence and the fluorescence of the sample. (c) Schematic representation of the lamellar hybrid phase. (b) X-ray spectra of the mixture of (DMPC/DMTAP 95:5) SUV+ and QD_{600}-**4** (5 μM) at room temperature (bottom) and at 40 °C (top). The peaks indicate a lamellar phase and a QDs superstructure. (d) X-ray spectra of the mixture of (DMPC/DMTAP 90:10) SUV+ and QD_{545}-**4** (bottom) or QD_{600}-**4** (top). Note the shift of the peak position with the QD size.

proposed in Figure 6c. The same specimens as shown in Figure 6a are observed by TEM after cryofracture. This well-established technique is well suited for the characterization of soft matter, like lipid phases or gels.[36] At low magnification (see Supporting Information, Figure E), the lamellar structure of the samples is clearly visible, with steps between bilayers that are visible in Figure 7a. The fracture occurs along the planes of the weakest resistance, i.e., between the two leaflets of the lipid bilayer. Additionally, the surface of the lamellae exhibits deformations that seem to be periodically oriented in some areas, as shown in Figure 7b. As a control experiment, in the case of the pure lipid lamellar system without QD, the surface of the lamellae appears flat (see Figure 7c). Therefore, these deformations are attributed to the presence of QDs, in agreement with the model proposed in Figure 6c. Another interesting feature can be observed when Figure 7b is carefully observed at the glancing angle. The packing of the QDs appears to be periodically arranged, with a periodicity of about 10 nm. The ordered areas are of small surface areas; therefore, no peaks are observed in the SAXS pattern. In conclusion, the membrane deformations clearly observed in freeze-fracture TEM pictures confirm the model presented in Figure 6c.

This model implies that the lamellar phase is presenting wide undulations induced by the strong electrostatic adhesion of the membranes around the QDs. Such mechanical deformation has never been observed with any other polyelectrolytes besides actin and DNA. The deformation energy of the membrane increases as d^{-4}, where d is the deformation wavelength.[37] Since the diameter of the QDs is larger than the DNA diameter by a factor 4, the deformation energy is reduced by a factor of around 256. The undulations are thus not mechanically forbidden, as their maximal amplitudes are about half the QD diameter: $d_{QD}/2$, e.g., 4−4.5 nm.

As observed in the case of DNA/cationic lipid complexes,[30,38] long-range order is expected to be observed with spherical colloids embedded within membranes and to produce interaction peaks between QDs on X-ray patterns. In the first studied samples, no interaction was observed, indicating the absence of any long-range positional order between QDs. In contrast, this can be achieved by reducing the QDs excess to 1 μM. In such case, an additional peak at 0.057 $Å^{-1}$ (Table 2, entry 5) appears. The same additional peaks are observed by decreasing the cationic charge density of the vesicle surface DMPC/DMTAP (95:5), as shown in Figure 6b (Table 2, entry 6). The corresponding interaction distance is about 11−12 nm and could be attributed to the distance between QDs. Indeed, this distance increases with the lipid surface through the L_β−L_α chain transition.

In conclusion, highly concentrated cationic SUV+ of different lipid mixtures burst in contact with anionic coated QD-**4** to form a multilayer composite phase of QDs embedded within bilayers. The membranes are strongly corrugated by electrostatic adhesion on the spherical coated QDs (Figure 8), and the positional order between spherical QDs can be modulated by the lipid mixture.

Conclusion

The synthesis of small, water-soluble quantum dots was successfully achieved from simple small peptides. These small, water-soluble, peptide-functionalized QDs possess optical and colloidal properties (size, charge, stability, etc.) that allow them to label and to target membrane vesicles. Depending on the size and the chemical composition of their surface, nanoparticles interact with the membrane in different manners. It was previously shown that the adhesion of micrometer-range latex particles onto lipidic membranes results in the partial or total wrapping of the particle.[39,40] Such phenomena are commonly

(36) Diaz, N.; Simon, F.-X.; Schmutz, M.; Rawiso, M.; Decher, G.; Jestin, J.; Mésini, P. *Angew. Chem., Int. Ed.* **2005**, *44*, 3260–3264.
(37) De Gennes, P.-G., Prost, J., *The Physics of Liquid Crystals* Oxford Science Publications ed.; Oxford, 1995.
(38) Salditt, T.; Koltover, I.; Rädler, J. O.; Safinya, C. R. *Phys. Rev. Lett.* **1997**, *79*, 2582–2585.
(39) Aranda-Espinoza, H.; Dan, Y. C., N.; Lubensky, T. C.; Nelson, P.; Ramos, L.; Weitz, D. A. *Science* **1999**, *285*, 394–397.

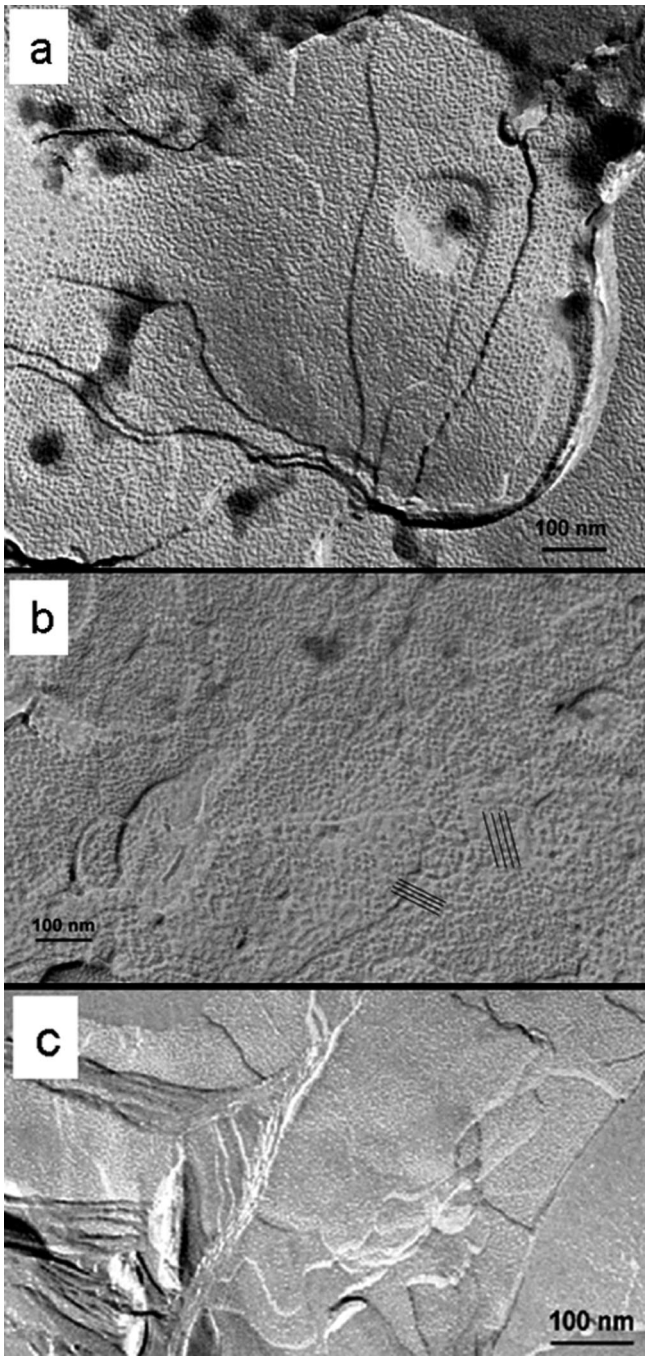

Figure 7. Freeze-fracture transmission electron microscopy images of a mixture of DMPC/DMTAP (90:10) SUV+ (a,b) in the presence or (c) in the absence of QD_{545}-**4**. Note the regular deformation of the membrane due to the presence of QDs and the packing of QDs appearing with an spacing of 8−12 nm.

observed in cells. It was also reported that nanosized particles such as QDs bound to specific peptidic receptors can enter into the cell by endocytosis.[6,41] The occurrence of non-endocytosis pathways has been recently investigated and is still an open question. Here, the QDs were found to strongly adhere to the vesicle surface. Their adhesion appears to be limited by the steric repulsion between QDs adhered on the surface. This process results in the formation of hybrid vesicles composed of one densely packed QD layer on the membrane's outer leaflet. These hybrid vesicles may be used as membrane nanoprobes and to transport nanoparticles into cells. Rupture occurs in the case of small vesicles, whereas the giant vesicles appear to be stable with the QD layer deposited on the membrane. In the case of small unilamellar vesicles, a condensed lamellar phase presenting a repeat distance between QDs is observed by SAXS and electron microscopy. In this condensed lamellar phase, the membrane is corrugated, probably to maximize the electrostatic interaction with QDs. Our self-assembling method is general and can be, in principle, extended to any type of charged, water-soluble nanoparticles (metallic, magnetic). By adjusting the distance between QDs in such self-organized hybrid structures, it might be possible to couple the optical properties of the nanocrystals and thereby develop new optical materials.

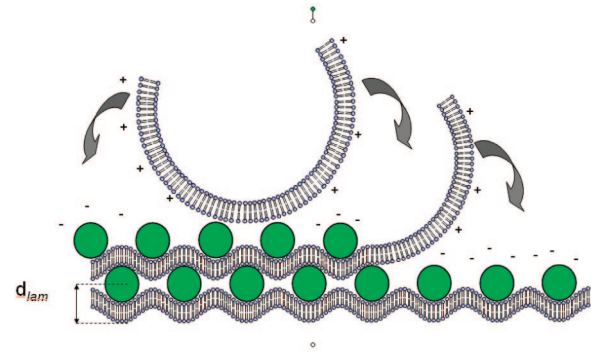

Figure 8. Schematic representation of the interaction between QDs and small vesicles resulting in the formation of the hybrid undulated lamellar phase.

Acknowledgment. The authors acknowledge financial support from the National Agency for the Research (ANR PNANO), the Région Bretagne, and Rennes Métropole. V.M.-A. and A.D. acknowledge the Région Bretagne for the Ph.D. fellowship of A.D. Dr. P. Schultz is deeply acknowledged for the use of the cryofracturing apparatus developed by Dr. J.-C. Homo at the IGBMC UMR 7104, Illkirch. M.D. acknowledges financial support from Fondation pour la Recherche Médicale (FRM). Drs. N. Messaddeq and Y. Schwab (IGBMC-Illkirch) are acknowledged for the access of their EM used for Figure 7c.

Supporting Information Available: Experimental details, including the synthesis of the peptides; Figure A, SE-HPLC spectra before and after purification of peptide-coated QD-**4**; Figure B, photostability and colloidal stability of a solution of QD-**4** under increasing ionic force; Figure C, zeta potential measurements during the titration of a solution of vesicle (LUV+) twice more concentrated than that in Figure 4a; Figure D, X-ray spectra of the mixture of (DMPC/DMTAP) SUV+ and QD_{600}-**4** (5 μM) containing various ratio r of positive charges (DMTAP) to negative nanoparticles ($r = n_{DMTAP}/n_{QD}$); Figure E, freeze-fracture TEM images of a mixture of QD_{545}-**4**/(DMPC/DMTAP 90/10) SUV+ with a large scale, demonstrating the multilamellar structure. This information is available free of charge via the Internet at http://pubs.acs.org.

JA711378G

(40) Ramos, L.; Lubensky, T. C.; Dan, N.; Nelson, P.; Weitz, D. A. *Science* **1999**, *286*, 2325–2328.
(41) Rajan, S. S.; Vu, T. Q. *Nano Lett.* **2006**, *6*, 2049–2059.